This article was downloaded by:
On: *26 January 2011*
Access details: *Access Details: Free Access*
Publisher *Taylor & Francis*
Informa Ltd Registered in England and Wales Registered Number: 1072954 Registered office: Mortimer House, 37-41 Mortimer Street, London W1T 3JH, UK

Liquid Crystals
Publication details, including instructions for authors and subscription information:
http://www.informaworld.com/smpp/title~content=t713926090

Self-assembly of twin tapered bisamides into supramolecular columns exhibiting hexagonal columnar mesophases. Structural evidence for a microsegregated model of the supramolecular column

Goran Ungar[a]; Darija Abramic[a]; Virgil Percec[b]; James A. Heck[b]
[a] Department of Engineering Materials and Center for Molecular Materials, The University of Sheffield, Sheffield, England [b] The W. M. Keck Laboratories for Organic Synthesis, Department of Macromolecular Science, Case Western Reserve University, Cleveland, OH, U.S.A.

To cite this Article Ungar, Goran , Abramic, Darija , Percec, Virgil and Heck, James A.(1996) 'Self-assembly of twin tapered bisamides into supramolecular columns exhibiting hexagonal columnar mesophases. Structural evidence for a microsegregated model of the supramolecular column', Liquid Crystals, 21: 1, 73 — 86
To link to this Article: DOI: 10.1080/02678299608033797
URL: http://dx.doi.org/10.1080/02678299608033797

PLEASE SCROLL DOWN FOR ARTICLE

Full terms and conditions of use: http://www.informaworld.com/terms-and-conditions-of-access.pdf

This article may be used for research, teaching and private study purposes. Any substantial or systematic reproduction, re-distribution, re-selling, loan or sub-licensing, systematic supply or distribution in any form to anyone is expressly forbidden.

The publisher does not give any warranty express or implied or make any representation that the contents will be complete or accurate or up to date. The accuracy of any instructions, formulae and drug doses should be independently verified with primary sources. The publisher shall not be liable for any loss, actions, claims, proceedings, demand or costs or damages whatsoever or howsoever caused arising directly or indirectly in connection with or arising out of the use of this material.

LIQUID CRYSTALS, 1996, VOL. 21, NO. 1, 73–86

Self-assembly of twin tapered bisamides into supramolecular columns exhibiting hexagonal columnar mesophases. Structural evidence for a microsegregated model of the supramolecular column

by GORAN UNGAR and DARIJA ABRAMIC
Department of Engineering Materials and Center for Molecular Materials, The University of Sheffield, Sheffield, S1 3DU, England

VIRGIL PERCEC* and JAMES A. HECK
The W. M. Keck Laboratories for Organic Synthesis, Department of Macromolecular Science, Case Western Reserve University, Cleveland, OH 44106-7202, U.S.A.

(*Received 25 August 1995; accepted 8 February 1996*)

The 1,2-bis[3,4,5-tris(alkan-1-yloxy)benzamido]ethanes (**DA-*n***, where n is the number of carbons in the alkanyl group) form a high temperature hexagonal columnar (Φ_h) liquid crystalline phase when $n=10$, 11, 12, 14, 16 and 18. **DA-*n*** with $n=4$, 5, 6, and 7 show at elevated temperatures a distorted hexagonal crystal phase. X-ray diffraction data support a model for the Φ_h phase consisting of a 2-D hexagonal lattice of self-assembled supramolecular columns in which the melted outstretching alkyl chains of **DA-*n*** occupy a space of constant density surrounding a rigid amide channel. A local ABAB stacking of layers along the column is proposed. Each layer contains two **DA-*n*** molecules. Layer B is rotated by 90° around the column axis relative to layer A. H-bonding between the amide groups is responsible for this mode of self-assembly.

Downloaded At: 09:01 26 January 2011

1. Introduction

Self-assembly of supramolecular architectures [1, 2] with well-defined shapes via various molecular recognition processes represents one of the most active topics of research in the area of supramolecular chemistry. A subject of particular interest in this field is the design of well-defined supramolecular shapes which in turn, generate assemblies exhibiting various liquid crystalline phases [3–6].

We are concerned with the design of different classes of molecular [7], macromolecular [8] and supramolecular architectures [9, 10] which display hexagonal columnar (Φ_h) mesophases. Hexagonal columnar mesophases are the most frequently encountered liquid crystalline phases exhibited by biological systems [11] and the least investigated in the field of synthetic liquid crystals [12]. Well-defined H-bonding interactions which have generated supramolecular columns displaying Φ_h phases were first elaborated by Lehn *et al.* [1(j), 4(*a*), (*b*)]. A supramolecular columnar liquid crystalline phase is not formed by discotic molecules [12(*a*)], or by main chain macromolecules [11(*a*), 12(*d*)], but rather by supramolecular discs (or strata) which are themselves self-assembled from a number of molecules. In previous publications from our laboratories, we have reported on the use of various combinations of molecular recognition processes based on ionic, dipolar, electrostatic and H-bonding interactions as well as polymerization reactions to self-assemble supramolecular columns [9, 10]. Based on accumulated empirical evidence, three essential criteria for self-assembly of such supramolecular columns have emerged. (*a*) The taper angle must be within appropriate limits: too low an angle results in smectic and, as recent experiments indicate, too high an angle may result in cubic phases. (*b*) Attractive interactions additional to van der Waals forces must exist at the apex of the molecule. In the cases studied, this was provided by one or several of the following: electrostatic interactions, H-bonding, covalent bonding (polymers), or complexation. (*c*) At the required temperature the wide end of the molecule must provide sufficient flexibility to enable effective decoupling of longitudinal register

*Author for correspondence.

0267–8292/96 $12·00 © 1996 Taylor & Francis Ltd.

between neighbouring columns, thus disallowing three-dimensional translational order. (*d*) In addition, amphiphilic character or any tendency for intramolecular phase separation appears to facilitate self-assembly. In the proposed general structure of self-assembled columns, tapered molecules are positioned with their apices near the column centre and with their wide ends consisting of melted alkyl groups at the periphery. In other words a microsegregation of the inner core and of the outer melted layer is assumed to generate the column. This model has so far been supported mainly by comparisons of columnar X-ray spacings with molecular models, as well as by the dependence of column stability on chemical structure and on the content of electrostatic, H-bonding or other stabilizing forces [9, 10].

The first goal of this paper is to verify this general model by comparing structural and thermal characteristics of an extensive series of column-forming tapered compounds in which the alkyl chain length is systematically varied from 1 to 18 carbon atoms. This will allow determination of the critical chain length necessary for the breakdown of 3-D translational order and *to test the hypothesis of a clean microphase separation between the aromatic amide core and the aliphatic outer sheath of constant density*. The second goal is to examine the specific effect of H-bonding on column structure and stability. This study is performed with the twin tapered bisamides 1,2-bis[3,4,5-tris(alkan-1-yloxy)benzamido]-ethanes (**DA-*n***, where *n* is the number of carbons in the alkanyl group).

Downloaded At: 09:01 26 January 2011

2. Experimental

2.1. *Materials*

1-Bromoundecane (98 per cent), 1-bromodecane (98 per cent), tetrabutylammonium hydrogen sulphate (TBAH, 97 per cent), toluenesulphonyl chloride (TsCl, 98 per cent), propyl gallate (98 per cent), 1-bromohexane (98 per cent), 3,4,5-tris(methoxy)benzoic acid (99 per cent) (all from Aldrich), 1-bromohexadecane (97 per cent), 1-bromotetradecane (97 per cent), 4-dimethylaminopyridine (DMAP, 98 per cent) (all from Fluka), 1,2-diaminethane (98 per cent) and ethylene glycol (Fisher), 1-bromobutane and diethylene glycol (Pfaltz & Bauer), and the other conventional reagents were used as received. Tetrahydrofuran (THF) was distilled from $LiAlH_4$. Triethylamine (Et_3N) was refluxed overnight over KOH, distilled, and then stored over KOH.

2.2. *Techniques*

^1H NMR (200 MHz) spectra were recorded on a Varian XL-200 spectrometer, at 20°C using TMS as an internal standard. Infrared (IR) spectra were recorded on a Perkin–Elmer 1320 infrared spectrometer (films obtained from $CHCl_3$ solution on KBr plates). A Perkin Elmer DSC-7 differential scanning calorimeter was used to determine the thermal transitions which were determined as the maximum and minimum of their endothermic and exothermic peaks. The DSC was calibrated with zinc and indium. In all cases, heating and cooling rates were 20°C min^{-1} unless specified. For some samples the crystalline transitions from the first heating scan differ from those of the second and subsequent heating scans. The difference results from the slow formation of crystalline phases compared to the heating and cooling rate of 20°C min^{-1}. However, second and subsequent heating scans are identical. High pressure liquid chromatography (HPLC) was performed with a Perkin–Elmer Series 10 LC instrument equipped with an LC-100 column oven and a Nelson 900 series integrator data station. A set of 2 Polymer Laboratories PL gel columns of 5×10^2 and 10^4 Å and $CHCl_3$ as solvent (1 ml min^{-1}) were used. The measurements were made at 40°C using a UV detector. X-ray diffraction patterns were recorded using either a helium-filled flat plate wide angle (WAXS) camera or a pin-hole-collimated small angle (SAXS) camera. Ni-filtered CuK_α radiation was used. The samples were in the form of: (*a*) as received in the form of powder or (*b*) bulk samples in Lindemann thin-walled 1 mm capillaries cooled from the melt. The temperature stability of the X-ray heating cell was ±0·1°C. A Carl–Zeiss optical polarized microscope (magnification 100 ×) equipped with a Mettler FP82 hot stage and a Mettler FP80 central processor was used to observe the thermal transitions and to analyse the anisotropic textures. Densities were measured with a gradient column at 23°C. Thin layer chromatography (TLC) was performed with Kodak 13181 Chromagram sheets containing a fluorescent indicator and using $CHCl_3$ containing 1–5 per cent CH_3OH (v/v) as the eluent. Molecular models of the individual aromatic cores of the molecules were constructed with Alchemy III from Tripos Associates, Inc. Assembly of the cores into molecular arrangements as well as the addition of the alkyl tails to the cores was performed with CSC Chem3D Plus from Cambridge Scientific Computing, Inc. Standard bond angles, lengths, and van der Waal's radii were used. The models were constructed using a Macintosh IIci computer with 12 Mb of RAM.

2.3. *Synthetic procedures*

The scheme outlines the synthesis of all compounds.

2.3.1. *Synthesis of the 3,4,5-tris(alkan-1-yloxy)benzoic acids (**1-*n***)*

The synthesis and characterization of **1-4/1***, **1-5**, **1-7**, **1-12**, and **1-18** was reported previously [9(*c*)]. The benzoic acids **1-4**, **1-6**, **1-10**, **1-11**, **1-14**, and **1-16** were

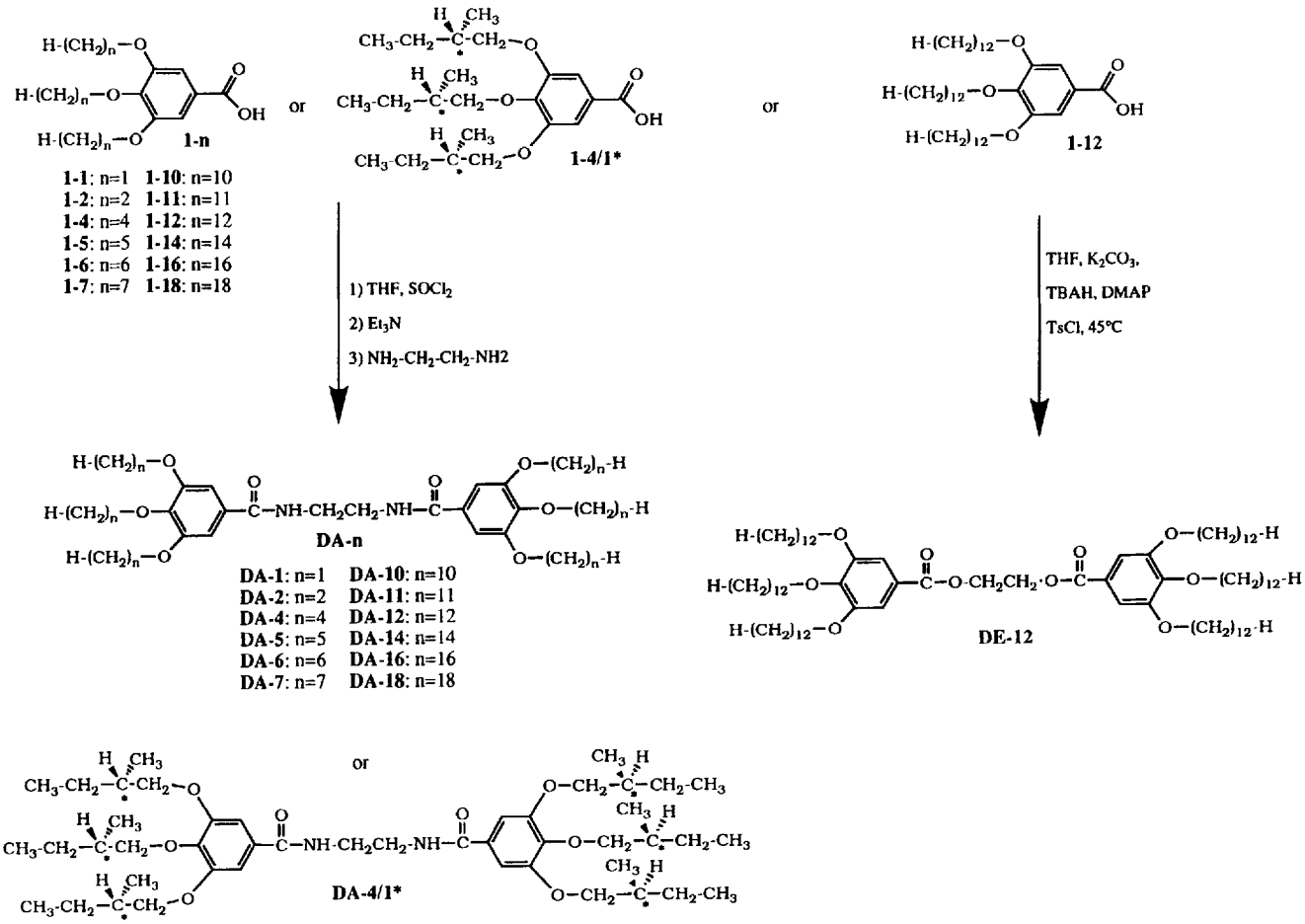

Scheme. The synthesis of 1,2-bis[3,4,5-tris(alkan-1-yloxy)benzamido]ethane (**DA-*n***), 1,2-bis{3,4,5-tris[*S*(-)-2-methylbutan-1-yloxy]benzamido}ethane (**DA-4/1***), and 1,2-bis[3,4,5-tris(*n*-dodecan-1-yloxy)benzoyloxy]ethane (**DE-12**).

synthesized according to the previously reported procedure by the etherification of the corresponding *n*-bromoalkane with propyl gallate in DMF using K_2CO_3 as base at 80°C under a N_2 atmosphere, followed by the hydrolysis of the ester group. All results are summarized in table 1. Compound **1-2** was synthesized as described below. The chemical shifts of the 1H NMR spectra of compounds **1-*n*** are reported in table 2. IR: *v* C=O, 1670–1675 cm^{-1}.

2.3.2. *Synthesis of 3,4,5-tris(ethan-1-yloxy)benzoic acid (1-2)*

A mixture of propyl gallate (11·46 g, 54 mmol), $(EtO)_2SO_2$ (19·8 ml, 180 mmol), K_2CO_3 (40 g, 290 mmol), TBAH (0·2 g, 0·6 mmol), and dry THF (100 ml) was refluxed for 12 h and then cooled to room temperature. The precipitated mixture of potassium salts was filtered out, and the solvent was evaporated. The resulting crude product was purified by column chroma-

Table 1. Synthesis of the 3,4,5-tris(*n*-alkan-1-yloxy)benzoic acids **1–4**, **1–6**, **1–10**, **1–11**, **1–14**, and **1–16**.

Compound	*n*	Propyl gallate/ mmol	1-Bromoalkane/ mmol	**1 – *n*** Yield/per cent	m.p./°C
1–4	4	120	365	51	65–67
1–6	6	47	157	72	38–40
1–10	10	47	144	71	53–54
1–11	11	42	128	73	53–55
1–14	14	34	108	54	69–70
1–16	16	79	365	57	78–80

Downloaded At: 09:01 26 January 2011

Table 2. ^{1}H NMR chemical shifts of compounds **1–2**, **1–4**, **1–6**, **1–10**, **1–11**, **1–14**, **1–16** and **DA-*n***.

Compound	Chemical shift (ppm, δ)
1–2	1·41 (overlapped peaks, 9 H, $-CH_3$), 4·14 (overlapped peaks, 6 H, $-CH_2-O$), 7·34 (s, 2 H, ArH)
1–4	0·99 (overlapped peaks, 9 H, $-CH_3$), 1·52 (overlapped peaks, 6 H, CH_3-CH_2-), 1·79 (overlapped peaks, 6 H, CH_2-CH_2-O-), 4·04 (t, 6 H, $-CH_2-O$), 7·34 (s, 2 H, ArH)
1–6	0·86 (t, 9 H, $-CH_3$), 1·26 (m, 18 H, $-(CH_2)_n-$), 1·75, (m, 6 H, $-CH_2-CH_2-O$), 3·97 (t, 6 H, $-CH_2-O$), 7·33 (s, 2 H, ArH)
1–10, 1–11 **1–14, 1–16**	The chemical shifts are the same as those of **1–6** with exception of the expected increase in the height of the peak at 1·28 ppm $[-(CH_2)_n-]$ associated with the increase in tail length
DA-1	3·70 (s, 4 H, $-CH_2-NH$), 3·89 (s, 18 H, $-CH_3-O$), 7·04 (s, 4 H, ArH), 7·15 (s, 2 H, NH)
DA-2	1·38 (overlapped peaks, 18 H, $-CH_3$), 3·65 (s, 4 H, $-CH_2-NH$), 4·08 (overlapped peaks, 12 H $-CH_2-O$), 7·04 (s, 4 H, ArH), 7·32 (s, 2 H, NH)
DA-4	0·91 (overlapped peaks, 18 H, $-CH_3$), 1·45 (overlapped peaks, 12 H, CH_3-CH_2-), 1·71 (overlapped peaks, 12 H, CH_2-CH_2-O-), 3·56 (s, 4 H, $-CH_2-NH$), 3·99 (t, 12 H, $-CH_2-O$), 7·03 (s, 4 H, ArH), 7·52 (s, 2 H, NH)
DA-4/1*	0·90 (t, 18 H, CH_3-CH_2-CH-*), 1·00 (d, 18 H, CH_3-CH-*), 1·22, 1·58, 1·78 (3m, 18 H, CH_3-CH_2-CH-*), 3·61 (s, 4 H, $-CH_2-NH$), 3·76 (s, 12 H, $-CH_2-O$), 7·00 (s, 4 H, ArH), 7·37 (s, 2 H, NH)
DA-5	0·87 (t, 18 H, $-CH_3$), 1·38 (m, 24 H, $-(CH_2)_n-$), 1·76 (m, 12 H, $-CH_2-CH_2-O$), 3·60 (s, 4 H, $-CH_2-NH$), 3·94 (t, 12 H, $-CH_2-O$), 6·98 (s, 4 H, ArH), 7·27 (s, 2 H, NH)
DA-6	0·86 (t, 18 H, $-CH_3$), 1·28 (m, 36 H, $-(CH_2)_n-$), 1·71 (m, 12 H, $-CH_2-CH_2-O$), 3·57 (s, 4 H, $-CH_2-NH$), 3·91 (t, 12 H, $-CH_2-O$), 7·02 (s, 4 H, ArH), 7·53 (s, 2 H, NH)
DA-7 to **DA-18**	The chemical shifts are the same as those of **2–6** with exception of the expected increase in the height of the peak at 1·28 ppm $[-(CH_2)_n-]$ associated with the increase in tail length. The NH peak varies between 7·11–7·42 ppm
2-12-EO	0·89 (t, 18 H, $-CH_3$), 1·25 (m, 108 H, $-(CH_2)_n-$), 1·76 (m, 12 H, $-CH_2-CH_2-OAr$), 3·97 (t, 12 H, $-CH_2-OAr$), 4·62 (s, 4 H, $-CH_2-OOCAr$), 7·25 (s, 4 H, ArH)

tography [silica gel, hexane containing 5 per cent ethyl acetate (v/v) as eluent]. The ester was hydrolysed by refluxing with 1 M KOH in EtOH (200 ml) for 30 min. The mixture was cooled and slowly acidified with dilute aqueous HCl. H_2O (1000 ml) was added and the resulting precipitate was filtered. The solid was dissolved in MeOH (20 ml) and precipitated into H_2O (200 ml). The solid was filtered and dried under vacuum to yield the white solid **1-2** (1·54 g, 11 per cent). HPLC: 99 per cent, m.p. 108–110°C.

2.3.3. *Synthesis of 1,2-bis[3,4,5-tris(alkan-1-yloxy)-benzamido]ethanes (**DA-n**)*

All **DA-*n*** compounds were synthesized by the general procedure described below. To a solution of **1-1** (1·53 g, 7·21 mmol) in dry THF (20 ml) was added dropwise $SOCl_2$ (0·52 ml, 7·17 mmol) followed by dry Et_3N (3·00 ml, 21·5 mmol) with stirring. The mixture was then added dropwise to a solution of 1,2-diaminoethane (0·30 ml, 4·49 mmol) in THF (15 ml) with stirring. The reaction mixture was heated at 40°C for 16 h, and then allowed to cool to room temperature. Then it was poured into H_2O (150 ml) and the resulting white precipitate was filtered. After five recrystallizations from MeOH [100 ml containing 5 per cent (v/v) $CHCl_3$] 0·55 g, 34 per cent of **DA-1** were obtained. The results of the syntheses of all **DA-*n*** are summarized in table 3. Their structure was confirmed by ^{1}H NMR analysis (see table 2), which also suggest a purity of about 100 per cent for all compounds [absence of the peaks associated with aliphatic amines (t, 2·8 ppm, CH_2-NH_2) and unreacted **1-1** (s, 7·31 ppm, Ar*H*–COOH)]. This purity was also supported by IR analysis [absence of unreacted **1-1** (ν C=O 1670 cm^{-1} for ArCOOH) and acid anhydride of **1-1** (ν C=O 1765 cm^{-1}), and the presence of the correct peaks for the amide group (ν C=O 1620 cm^{-1}, ν N–H 3200 cm^{-1})]. The frequency of the non-H-bonded amide peaks are: ν C=O 1680 cm^{-1}, ν N–H 3450 cm^{-1}: The density of **DA-12** at 23°C is 0·98 g cm^{-3}.

2.3.4. *Synthesis of 1,2-bis[3,4,5-tris(n-dodecan-1-yloxy)benzoyloxy]ethane (**DE-12**)*

DE-12 was synthesized and purified according to a previously reported procedure [9(*e*)].

From **1-12** (2·0 g, 3·00 mmol) and ethylene glycol (0·09 g, 1·5 mmol) **DE-12** was obtained as a white powder (1·21 g, 59 per cent). HPLC: 99 per cent, m.p. 63°C (DSC, 20°C min^{-1}), IR: ν C=O 1705 cm^{-1}. The results of the NMR characterization are reported in table 2.

2.4. *X-ray diffraction experiments*

X-ray diffraction experiments were performed both during heating of the crystalline sample from room temperature into the isotropic melt and while cooling back to room temperature. During cooling, all **DA-*n*** samples spontaneously oriented so that it was possible to distinguish equatorial ($h\,k$) reflections from meridional (l) reflections. The best X-ray diffraction patterns were

Downloaded At: 09:01 26 January 2011

Table 3. Synthesis of the 1,2-bis[3,4,5-tris(alkan-1-yloxy)benzamido] ethanes (**DA-*n***).

Compound	$-(CH_2)_nH$ n	$H_2N(CH_2)_2NH_2$ /mmol	RCOOH[a] /mmol	$SOCl_2$ /mmol	Et_3N /mmol	Recrystallization solvent/cosolvent	Yield/per cent
DA-1	1	4·5	7·2	7·2	21·5	MeOH/$CHCl_3$	34
DA-2	2	7·5	11·8	11·2	35·9	MeOH	25
DA-4	4	11·8	11·8	11·7	35·9	MeOH	53
DA-4/1*	4/1	4·2	4·2	4·3	14·3	MeOH	30
DA-5	5	7·8	7·9	7·9	28·7	MeOH	21
DA-6	6	4·6	9·5	9·4	21·5	MeOH	25
DA-7	7	3·0	6·5	6·2	14·3	EtOH	30
DA-10	10	2·5	5·1	5·1	14·3	EeOH	73
DA-11	11	6·3	6·3	6·2	28·7	EtOH/$CHCl_3$	57
DA-12[b]	12	150·0	14·8	15·2	15·8	–	36
DA-14	14	5·2	5·3	5·2	28·7	Acetone/$CHCl_3$	75
DA-16	16	2·2	4·7	4·7	21·5	Acetone/THF	70
DA-18	18	1·8	3·2	3·3	7·2	Acetone/THF	46

[a] $1-n$ with the number of methylenic units in the tails equal to n in column 2. [b] The monosubstituted amine was the intended product. The product was purified by column chromatography with silica gel and $CHCl_3$ as the eluent.

Downloaded At: 09:01 26 January 2011

obtained from samples cooled slowly from the isotropic phase. The cooling rate of 6°K h^{-1} was usually adequate for high diffraction orders of the columnar phase to develop.

Single crystals of **DA-1** were generated by recrystallization from MeOH containing 5–10 per cent $CHCl_3$ and dried at 10^{-1} mmHg for 24 h. The crystal structure was determined and is summarized in figure 1. The position of the molecules in the unit cell is shown in figure 1 (*a*). The angles and lengths associated with the H-bonding in the crystalline phase are shown in figure 1 (*b*). Specific details of the crystal structure and atomic coordinates will be published elsewhere [13]. Single crystals from the diamides with longer alkyl tails could not be obtained with adequate perfection.

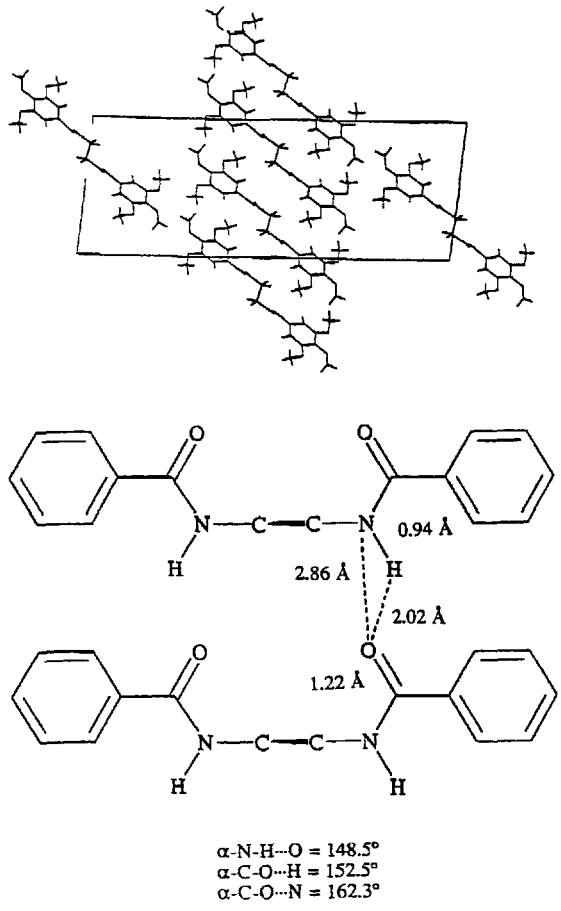

Figure 1. Summary of the molecular structure and most significant distances of the crystal structure of **DA-1.**

3. Results and discussion

3.1. *Synthesis*

The scheme outlines the synthesis of **DA-*n*** and of the model compound **DE-12**. All diamides **DA-*n*** were obtained from the corresponding acids **1-*n*** via *in situ* formation of their acid chlorides followed by amidation with 1,2-diaminoethane. Compounds **1-*n*** were prepared by the alkylation of propyl gallate with the corresponding *n*-bromoalkanes as was described in the experimental part. The **DA-*n*** products were recrystallized 3 to 5 times until a single spot was observed by TLC and their melting points remained constant. In addition, ^{1}H NMR analysis demonstrated the absence of impurities.

3.2. *Characterization by differential scanning calorimetry*

The thermal transitions of compounds **DA-*n*** and **DE-12** were determined by DSC. The transition

temperatures and their corresponding enthalpies are summarized in table 4. The meaning of the short names of the various phases is explained in the caption of table 4. The two highest transition temperatures of the **DA-*n*** are plotted versus *n* in figure 2. All phases were characterized by X-ray diffraction to be discussed in detail in a subsequent section. With the exception of crystalline melting temperature (T_m) of **DA-4**, all transitions plotted in figure 2 were determined from the first DSC heating scans of solution-crystallized compounds. As *n* increases from 1 to 7, T_m of **DA-*n*** decreases sharply.

In addition to various crystalline phases, the diamides **DA-10** to **DA-18** display a hexagonal columnar liquid crystalline phase (Φ_h). The isotropization transition temperature (T_i) of the Φ_h mesophase decreases systematically with increasing *n*, but much less steeply than does the crystalline melting transition of the **DA-*n*** with $n < 10$.

Figure 3 shows the DSC traces of **DA-12** and of **DE-12**. These two compounds have quite similar chemical structures, shape, and polarity. However, **DE-12**

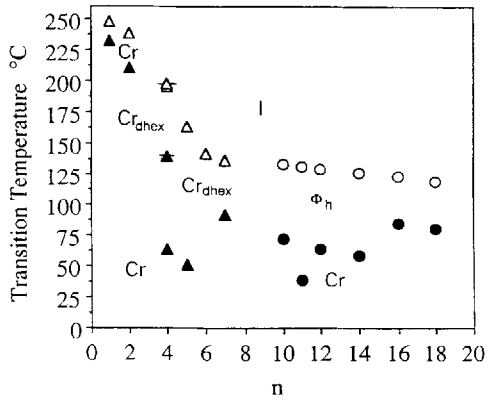

Figure 2. The dependence of selected transition temperatures of **DA-*n*** and **DA-4/1*** on the number of carbon atoms in the alkyl tail *n*. ▲ = crystal–crystal transition; △ = crystal melting (T_{cr-i}); ● = crystal–Φ_h transition ($T_{cr-\Phi h}$); ○ = hexagonal columnar–isotropic transition ($T_{\Phi h-i}$). -△- and -▲- are for **DA-4/1***.

Table 4. Thermal transitions of **DA-*n*** and **DE-12** (Φ_h = hexagonal columnar liquid crystalline mesophase; Cr_{dhex} = distorted hexagonal crystalline phase; Cr_{hex} = hexagonal crystalline phase; Cr_1, Cr_2, Cr_3 = crystalline phases; I = isotropic phase). The data on the first line are from the first heating and the first cooling DSC scans and data on the second line are from the second heating DSC scans.

Compound	Thermal transitions (°C) and the enthalpy changes (kJ mol^{-1} in parentheses)	
	Heating scan	Cooling scan
DA-1	Cr_2 232(3·77) Cr_1 248(81·64) I Cr_1 246(80·81) I	I 197(74·94) Cr_1 183(0·29) Cr_2
DA-2	Cr_3 126(15·07) Cr_2 210(0·67) Cr_1 238(51·92) I Cr_2 205(1·51) Cr_1 238(52·34) I	I 196(48·57) Cr_1 169(2·18) Cr_2
DA-4	Cr_{dhex} 195(55·27) I Cr_2 26(0·96) Cr_1 63(0·96) Cr_{dhex} 194(55·26) I	I 174 (53·17) Cr_{dhex} 51(1·26) Cr_1 17(1·13) Cr
DA-4/1*	Cr_2 139(7·54) Cr_1 198(45·22) I Cr_1 199(41·45) I	I 174(37·26) Cr
DA-5	Cr_2 −16(2·93) Cr_{hex} 51(6·99) Cr_{dhex} 163(37·68) I Cr_2 −16(3·06) Cr_{hex} 49(5·86) Cr_{dhex} 163(37·68) I	I 142(34·75) Cr_{dhex} 41(8·37) Cr_{hex} −26(2·55) Cr_2
DA-6	Cr_1 0(5·44) CR_{dhex} 141(43·96) I Cr_1 1(5·02) Cr_{dhex} 142(44·38) I	I 119(39·36) Cr_{dhex} −18(6·28) Cr_1
DA-7	Cr_1 92(54·01) Cr_{dhex} 136(38·94) I Cr_1 9(10·47) Cr_{dhex} 137(39·77) I	I 117 (36·43) Cr_{dhex} 0(11·30) Cr_1
DA-10	Cr_2 24(8·79) Cr_1 72(46·05) Φ_h 133(43·96) I Cr_3, Cr_2, Cr_1 4, 22, 25(35·59)[a] Φ_h 133(45·22) I	I 114(39·77) Φ_h 13, −9(33·49)[a] Cr_1, Cr_2
DA-11	Cr_2, Cr_1 16, 38(46·47)[a] Φ_h 131(44·80) I Cr_2, Cr_1 17, 38(50·66)[a] Φ_h 131(44·80) I	I 112(40·19) Φ_h 27, 4(54·43) Cr_1, Cr_2
DA-12	Cr_2, Cr_1 41, 63(93·37)[a] Φ_h 129(42·29) I Cr_2, Cr_1 38, 44(79·55)[a] Φ_h 129(42·29) I	I 110(39·36) Φ_h 32, 17(75·78)[a] Cr_1, Cr_2
DA-14	Cr_3, Cr_2, Cr_1 3, 43, 58(146·12)[a] Φ_h 126(45·64) I Cr_2, Cr_1 49, 58(104·67)[a] Φ_h 126(45·64) I	I 107(41·03) Φ_h 44, 38(109·69)[a] Cr_1
DA-16	Cr_2, Cr_1 72, 84(123·51)[a] Φ_h 123(45·22) I Cr_3 37(20·93) Cr_2, Cr_1 70, 74(111·37)[a] Φ_h 123 (43·54) I	I 106(41·45) Φ_h 54, 48(12·27)[a] Cr_1, Cr_2 −1(15·49) Cr_3
DA-18	Cr_1 55, 72, 80(182·96)[a] Φ_h 119(85·66) I Cr_3 54(1·76) Cr_2, Cr_1 74, 80(125·60)[a] Φ_h 118(39·36) I	I 104(38·94) Φ_h 64, 53, 44(133·98)[a] Cr_1, Cr_2, Cr_3
DE-12	Cr_2, Cr_1 31, 63(116·39)[a] I Cr_2 31(20·52) 42 (−17·17) Cr_1 61(73·69) I	I 16(87·09) Cr_1

[a] Combined enthalpies are presented for overlapped transitions.

Downloaded At: 09:01 26 January 2011

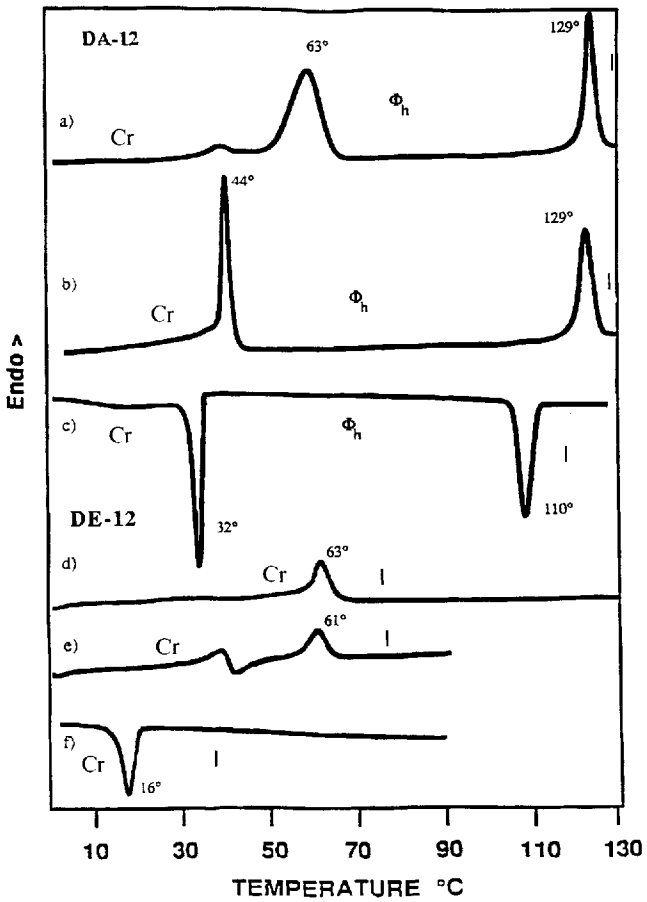

Figure 3. DSC traces ($20°C^{-1}\,min^{-1}$) of **DA-12**: (*a*) first heating scan, (*b*) second heating scan, (*c*), first cooling scan; and of **DE-12**: (*d*) first heating scan, (*e*) second heating scan, and (*f*) first cooling scan.

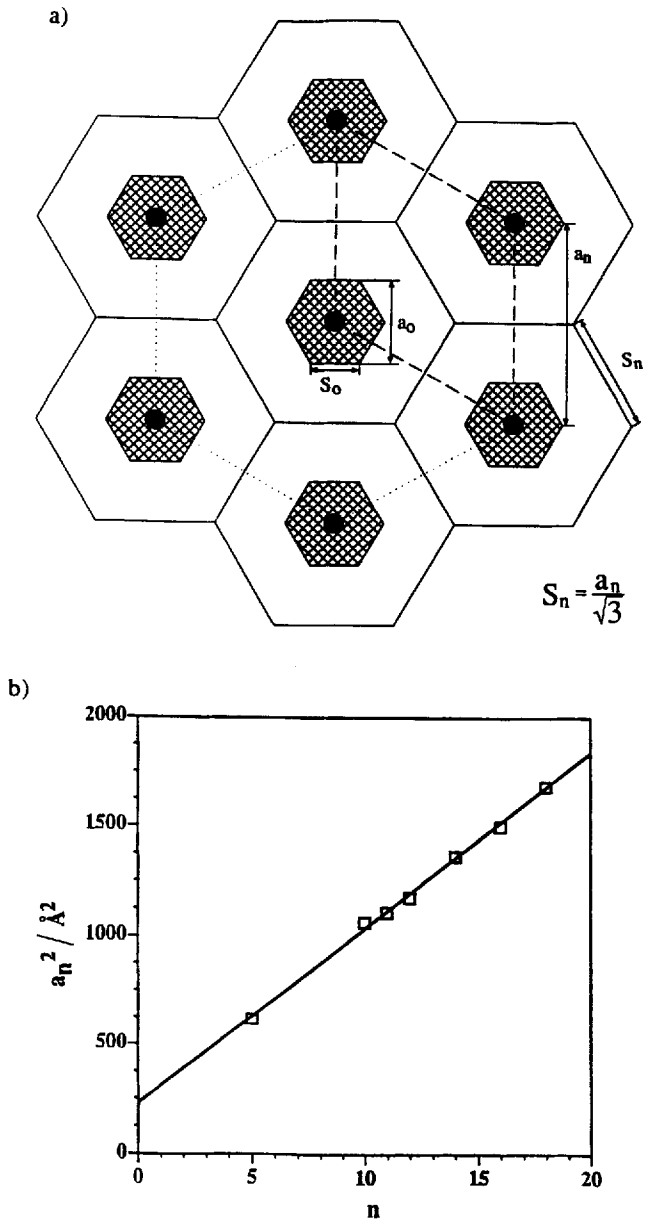

Figure 4. (*a*) Schematic representation of the columns in the Φ_h phase as viewed from the top, and the dimensions according to the X-ray scattering experiments; (*b*) extrapolation of equation (4) to $n=0$.

melts into an isotropic liquid while **DA-12** melts into a Φ_h mesophase which undergoes isotropization at 129°C. **DA-12** has both proton donor (NH) and proton acceptor (C=O) groups in its structure. **DE-12** has proton acceptor groups but does not have any strong proton donor groups in its structure. Consequently the **DA-12** (and all **DA-*n***) can self-H-bond in the bulk. **DE-12** can only form H-bonds if a second component containing a proton donor group is added. The results shown in figure 3 demonstrate that self-H-bonding inter- or intramolecularly is a favourable interaction for the formation and stabilization of the supramolecular structures responsible for the formation of the Φ_h mesophase.

3.3. *Polarized microscopy textures*

Compounds **DA-1** to **DA-7** display conventional crystalline spherulites upon cooling from the isotropic phase. When cooled only a few degrees below the beginning of the formation of the texture, the material can be sheared causing the spherulites to break. The diamides **DA-10** to **DA-12** exhibit fan shaped textures typical to Φ_h phase [7]. The texture forms by the appearance of many scattered bright areas which then grow upon slow cooling or annealing. Diamide **DA-14** forms only very few light areas. These areas do not grow upon annealing for 30 min or with further cooling. When observed between crossed polarizers, diamides **DA-16** and **DA-18** remain completely black (optically isotropic) upon cooling from the isotropic melt into the Φ_h phase. Shearing of the specimen does not induce birefringence. A possible

Downloaded At: 09:01 26 January 2011

Table 5. Observed and calculated X-ray reflections for **DA-10**, **DA-11**, **DA-12**, **DA-14**, **DA-16** and **DA-18** in the Φ_h phase.

Compound (and T/°C)		Spacing/Å											
	hkl	100	110	200	210	300	220	310	400	320	410	330	a_n
DA-10	obs	27·3	16·7	14·4	10·5	8·9	8·1		7·28	–	5·94	5·30	32·6
(104)	*calc*	*28·2*	*16·3*	*14·1*	*10·7*	*9·41*	*8·15*	*7·83*	*7·06*	*6·48*	*6·16*	*5·43*	± *1·0*
DA-11	obs	28·6	17·4	14·4	10·9	9·4	8·2		–	–	–	–	33·3
(95)	*calc*	*28·8*	*16·7*	*14·4*	*10·9*	*9·61*	*8·32*	*8·00*	–	–	–	–	± 0·7
DA-12	obs	30·7	16·8	14·8	11·0	9·9	–		–	–	–	–	34·3
(95)	*calc*	*29·7*	*17·2*	*14·8*	*11·2*	*9·90*	–	–	–	–	–	–	± 0·5
DA-14	obs	32·1	18·6	15·4	11·8	10·6	9·1		8·3	7·33	–		36·9
(95)	*calc*	*32·0*	*18·4*	*16·0*	*12·1*	*10·65*	*9·23*	*8·86*	*7·94*	*7·33*	–	–	± 0·7
DA-16	obs	33·4	19·6	16·7	12·6	11·2	–	–	–	–	–	–	38·7
(95)	*calc*	*33·5*	*19·4*	*16·7*	*12·7*	*11·2*	–	–	–	–	–	–	± 0·3
DA-18	obs	34·6	20·8	17·9	–	11·9	–	9·8				–	41·0
(95)	*calc*	*35·5*	*20·5*	*17·8*	–	*11·8*	*10·2*	*9·85*	–	–	–	–	± 0·7

Table 6. Observed and calculated X-ray reflections for **DA-5** in the Cr_{hex} phase at 20°C (hexagonal unit cell: $a = 24{\cdot}9$ Å, $c = 9{\cdot}4$ Å).

	Spacing/Å								
hkl	100	110	200	210	300	220	310	400	320
obs	22·1	12·6	10·8	8·2	7·11	6·24	5·98	5·30	4·98
calc	*21·6*	*12·5*	*10·8*	*8·15*	*7·19*	*6·23*	*5·98*	*5·39*	*4·95*
hkl	101	111	201	002	102	112	212	302	222/402
obs	8·4	7·55	7·05	4·78	4·55	4·46	4·10	3·97	3·80
calc	*8·61*	*7·50*	*7·08*	*4·70*	*4·59*	*4·40*	*4·07*	*3·93*	*3·75*
hkl	312	322	412	003	103	303	313		
obs	3·72	3·43	3·31	3·15	3·07	2·93	2·82		
calc	*3·70*	*3·41*	*3·32*	*3·13*	*3·10*	*2·87*	*2·78*		

Downloaded At: 09:01 26 January 2011

explanation of the fact that the columnar phase of **DA-16** and **DA-18** appears optically isotropic is that the contributions to the overall birefringence Δn arising from the central and peripheral areas of the column cancel. While the peripheral areas will have negative birefringence due to the radially oriented aliphatic chains, in order for this to be cancelled the column cores would have to have positive birefringence. This interpretation implies positive birefringence in the columnar phase of **DA-*n*** with shorter alkoxy tails.

3.4. *Characterization by X-ray diffraction experiments*

The diamides **DA-*n*** with $n = 4$, 4/1*, 5, 6, 7, 10, 11, 12, 14, 16, and 18 were characterized by X-ray diffraction experiments. These experiments have established that the high temperature phase of diamides with $n \geqslant 10$ is Φ_h. All sharp reflections could be indexed as $hk0$, and furthermore, in samples where preferred orientation was sufficiently developed all reflections were found to be equatorial. The observed reflections and their indices for the Φ_h phase of **DA-10**, **DA-11**, **DA-12**, **DA-14**, **DA-16**, **DA-18**, and of the hexagonal crystalline (Cr_{hex}) phase of **DA-5**, are summarized in tables 5 and 6. In most cases reflections 220 and 310 were found to overlap. In **DA-10** reflections of the order as high as $hkl = 330$ were observed. All diamides with $n \geqslant 10$ display a diffuse halo in the 4–5 Å range, characteristic of the liquid-like positional disorder out of the hexagonal lattice plane.

For a Φ_h liquid crystalline phase, the number of observed reflections is unusually high. In most columnar phases including those of discotic and phasmidic molecules, the number of observed sharp reflections rarely exceeds 5. The large number of reflections in the present compounds indicates a comparatively high **2-D** positional order parameter, i.e. a comparatively low 'thermal disorder'. With increasing alkyl tail length the number of observed reflections decreases, indicating an increased disorder.

The reflections of the **DA-5** at $T = 20$°C correspond to a 3-D hexagonal crystal lattice. Indexing was

facilitated by the considerable degree of preferred orientation obtained in the sample during cooling in the glass capillary tube from the isotropic melt. The dimensions and the volume of the unit cell are $a=24{\cdot}9$ ($\pm 0{\cdot}3$) Å, $c=9{\cdot}4$ ($\pm 0{\cdot}2$) Å and $V=5042$ (± 202) Å^3. Using the experimental macroscopic density value of $\rho=0{\cdot}98$ g cm^{-3}, the number of **DA-5** molecules per unit cell N was calculated as 3·8. Rounded to the nearest integer this gives $N=4$ **DA-5** molecules per unit cell.

In the high temperature phase of **DA-5** at $T=80$°C the general reflection pattern persisted but the $hk0$ reflections become split. The degree of orientation was insufficient to allow the determination of the unit cell of this lower symmetry form. The structure is denoted 'distorted hexagonal crystal' (Cr_{dhex}).

X-ray diffraction patterns of **DA-4**, **DA-6**, and **DA-7** in the phase below the isotropic phase are similar to those of the **DA-5** sample taken at 80°C. These structures were also assigned as k_{dhex}. Powder diffraction of **DA-4/1*** at 25°C shows a number of sharp wide-angle reflections. The crystalline structure persists up to the final melting point. The crystal structure of **DA-4/1*** is different from **DA-4**, **DA-5**, **DA-6**, and **DA-7** also in that no gross preferred orientation occurs during slow cooling from the isotropic phase.

Since the measurements on all diamides were not performed at exactly the same temperature, the possible temperature dependence of the alkyl chain lengths was experimentally tested on **DA-11** and gave $a_{11}=32{\cdot}7$ ($\pm 0{\cdot}1$) Å at $T=42$°C and $a_{11}=33{\cdot}0$ ($\pm 0{\cdot}2$) Å at $T=95$°C. Both values lie within the error of the measurement, and thus the effect of temperature can be neglected for the present purpose.

In further attempts to determine the structure of the columns in the liquid crystalline phase we tested a model in which a column is composed of an inner core of fixed width and an outer sheath of molten alkyl chains of uniform density ρ_o whose thickness varies with the length of the alkyl tail. As the unit cell is 2-D hexagonal, the columnar cross-section which allows for the space filling is a hexagon (see figure 4(*a*)). The parameter S_n, which is the length of the side of the cell of the columnar hexagon, is in the following relation with the measured parameter a_n of the 2-D hexagonal unit cell:

$$S_n = \frac{a_n}{(3)^{1/2}} \tag{1}$$

The volume V_n of a hexagonal prism representing a stratum of a hexagonal column of thickness d is

$$V_n = V_o + V_{alk} \tag{2}$$

where V_o and V_{alk} are the volumes of the central amide portion and of the outer alkyl sheath, respectively. The essence of the model is the constant density ρ_o of the alkyl region. Hence, since there are 6 alkyl chains of n carbon atoms per diamide, and N molecules per stratum:

$$V_{alk} = \frac{6N}{\rho_o}(m_H + nm_{CH_2}). \tag{3}$$

In equation (3) m_H and m_{CH_2} are the respective masses of a hydrogen atom and of a CH_2 group. As the volume of a hexagonal prism of side length S is (3/2) $(3)^{1/2}dS^2$, by dividing equation (2) with (3/2) $(3)^{1/2}d$, inserting in equation (3), and setting $(12N)/((3)^{1/2}d\rho_o) = A$ we obtain

$$S_n^2 = S_o^2 + \frac{A}{3}m_H + n\frac{A}{3}m_{CH_2} \tag{4a}$$

or

$$a_n^2 = a_o^2 + Am_H + nAm_{CH_2} \tag{4b}$$

A least squares fit of equation (4) was carried out for all **DA-n** ($n=10$, 11, 12, 14, 18) in the Φ_h phase, and for **DA-5** in the Cr_{hex} phase (see figure 4(*b*)). All the experimental points, including that for the crystalline **DA-5**, lie within the experimental error of the fitted line, which indicates that the model adopted is correct and that ρ_o is indeed constant. The linear dependence of the column diameter, or hexagonal lattice parameter a_n^2, on n (see figure 4(*b*)) is equivalent to the well-established 'log–log plot' method applied to lyotropic systems [12(*f*)]. In this last case a plot of log (X-ray spacing) versus log (solvent volume) indicates a 2-D columnar phase. Similarly, slopes of 1 or 3, respectively, indicate lamellar and cubic phases. The extrapolated value of 231 Å^2 for $n=0$ is equal to $a_o^2 + Am_H$. Since A, as obtained from the slope of the straight line in figure 4(*b*), is 80·3/14 Å^2/Dalton, $a_o = 15{\cdot}0$ Å and thus the diamide core dimension S_o is

$$S_o = \frac{a_o}{(3)^{1/2}} = \frac{15{\cdot}0}{(3)^{1/2}} = 8{\cdot}66 \text{ Å}. \tag{5}$$

The constant $A = (12N)/((3)^{1/2}d\rho_o$ contains the product of two unknowns, d and ρ_o. However, if a stratum of the column is defined as an averaged layer containing an integer number N of diamide molecules, then d, the thickness of that layer, can be determined independently from the measured macroscopic density ρ and the cross-sectional area of the column, according to $d = (2NM)/(3(3)^{\frac{1}{2}}N_A a_n^2 \rho)$. Molecular modelling strongly suggests that $N=2$ (see the following sections). Thus, for example for **DA-12** where $\rho=0{\cdot}98$ g cm^{-3}, a value for the structure thickness of $d=4{\cdot}6$ Å is obtained.

The density of the alkyl sheath ρ_o can now be calculated as $d = 24/(3)^{\frac{1}{2}}Ad$). ρ_o is obtained as 0·87 g cm^{-3}. This value is normally associated with the amorphous phase of polyethylene and it is higher than the value of 0·75 g cm^{-3} for pure n-alkane liquids. An independent

Downloaded At: 09:01 26 January 2011

test of the model and of the derived parameters is provided by the calculated core density being $\rho_{core} = 1{\cdot}19\,g\,cm^{-3}$, which is in the expected range.

3.5. *Crystal symmetry of the low-temperature phase of* ***DA-5***

Since the low temperature modification of **DA-5** turns out to be hexagonal, and since the hexagonal lattice parameter a of this phase fits well with the chain length dependence of the hexagonal columnar phases of **DA-*n*** with $n \geqslant 10$, any information on crystal packing in the **DA-5** crystals may be useful in elucidating the molecular arrangement in the columns of the Φ_h phase. While single crystal structure determination of **DA-5** could not be performed, it is still possible to derive limited conclusions on its structure by considering the space groups compatible with the diffraction data and by utilizing other information. Specifically, the following additional information narrowed the choice of lattice symmetry: (i) In accordance with experimental density, there are 4 molecules of **DA-*n*** per unit cell. (ii) The a-dimension of the unit cell fits well with that extrapolated for the columns of the Φ_h phase of the long alkyl tail diamides. This suggests a similar molecular arrangement in both cases. (iii) The c-dimension of the unit cell of 9·4 Å is of the order of 2 molecular thicknesses ('thickness' means the shortest molecular dimension). (iv) The absence of the 0 0 1 reflection but not of the other 0 0 1 reflections with 1 = odd, including 0 0 3, is seen as an indication that there may be 2 layers of molecules (A and B), with ABAB stacking in the c-direction, where layers A and B are similar but differ by more than just a simple glide plane or screw axis transformation. The details of the symmetry consideration of the **DA-5** structure are given in the Appendix. In summary, the most likely space group is $P6/m2/m2/m$, the symmetry reflecting that of the averaged unit cell of an orientationally and conformationally highly disordered crystal. The top view of the hexagonal unit cell is shown schematically in figure 5(*d*) with each full circle denoting 2 molecular pairs, one at elevation z and another at $-z$. A two-fold screw axis or glide plane along the unique axis (consequently, for example $z \neq 1/2$) is absent. The long-range persistence of pairing of non-equidistant layers in this otherwise highly disordered crystal phase is an interesting occurrence.

In broad terms, the crystalline phase of **DA-5** is a three-dimensional extension of molecular organization in the two-dimensionally ordered Φ_h phase. This serves to confirm the role of long conformationally disordered alkyl tails in the Φ_h phase formation by screening the periodic potential between columns. Thus for the diamides with $n \geqslant 10$, the 3D order breaks down, while

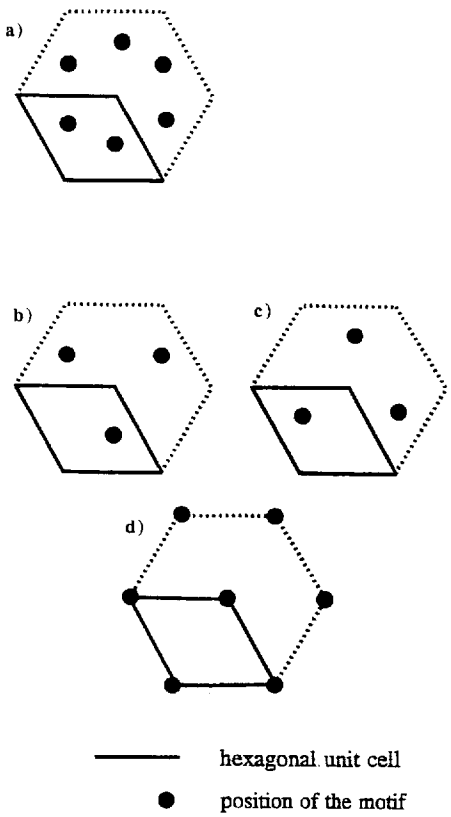

Figure 5. Possible spatial arrangements of the molecular pairs in a hexagonal packing.

for **DA-5** the shorter pentyl groups still preserve the intercolumnar registry.

3.6. *Molecular models*

Some further but more tentative conclusions about molecular arrangement of bisamide molecules can be drawn by considering molecular models. Because of the small number of bisamide molecules per column element and relative rigidity of their core regions, it turns out that only a few packing models remain feasible after taking account of the experimental data presented, of the possible H-bonding models and of the requirement for efficient space filling. We have constructed molecular models of the core of the columns based on different possible conformations and H-bonding motifs. Information on the strength and geometry of H-bonds for amides is available in the literature [14(*a*)–(*m*)]. We have taken account of literature data on H-bonds of amides when evaluating the feasibility of possible **DA-*n*** conformations. **DA-*n*** molecules have a reduced H-bond number [14(*b*)] (R) of two. This means the maximum number possible for simple 1:1 H-bonds that can be formed per **DA-*n*** molecule is two. Three and four centre H-bonds were also considered. The average distance for

Downloaded At: 09:01 26 January 2011

H··O contacts in the H-bond derived from amides is 1·9 Å [14(*f*)]. The ranges of optimum angles for N–H··O and H··O–C bonds are 159–172° [14(*d*), (*f*), 15(*a*)] and >90° [14(*f*)] respectively.

Crystal structures of related compounds have also been taken into consideration [15]. In a different study which is related to the present one, 1,3-bis[3,5-bis(*n*-alkan-1-yloxy)benzamido]-2,4,6-trimethylbenzenes with alkyl tail lengths of 10, 11, and 12 methylenic units displayed a Φ_h mesophase just below a nematic mesophase [16]. The packing of the molecules within the column was suggested to be based on a helical arrangement. However, no details on the possible placement of the molecules within the column were provided.

Utilizing this information we were able to arrive at two possible models of columnar packing of **DA-*n*** molecules. Arrangements which were based upon a single intramolecular H-bond [14(*f*), (*m*)] resulting from a gauche or skew conformation of the ethylenic spacer were dismissed because of intra- and intermolecular steric hindrance. Association of two molecules to form a H-bonded disc is also dismissed because it results in 50 per cent of available groups being unable to form H-bonds.

Figure 6(*a*) shows schematically one possible arrangement of **DA-*n*** molecules which could adequately satisfy the requirements necessary to form a Φ_h mesophase based on the information we have presented in the preceding sections. It is based on 2 molecules of **DA-*n*** placed side-by-side within a cross-section layer of the column. Each parallelepiped represents one **DA-*n*** molecule and the connecting vertical lines schematically represent the H-bonds. H-bonding is completely intermolecular and is directed along the column axis between adjacent molecules. One problem with this model is with some overcrowding of aliphatic chains in the direction parallel to the long axis of bisamide molecules, and with a corresponding underoccupancy in the transverse direction.

The latter problem is aleviated in the second model, schematically depicted in figure 6(*b*). It differs from model 1 in that the molecular pairs of adjacent layers are rotated by 90° around the column axis. H-bonds are again directed vertically along the column axis, but the column is now interlinked entirely by a H-bond network. The aliphatic chains are more evenly distributed around the column core. Figures 7(*a*) and (*b*) show the top and side views of a possible molecular arrangement of the column core corresponding with the model in figure 6(*b*). In order for the H-bonding contacts to be formed between adjacent layers, the amide groups of the two different molecules within a layer on the same side of the column axis must be approximately 4·3 Å away from each other. This distance results from averaging the covalent spacing of the carbonyl O atoms with the covalent spacing of the H atoms on the N atom in a single molecule. For this distance to be achieved the aromatic rings must be tilted to prevent strong intermolecular repulsive steric interactions.

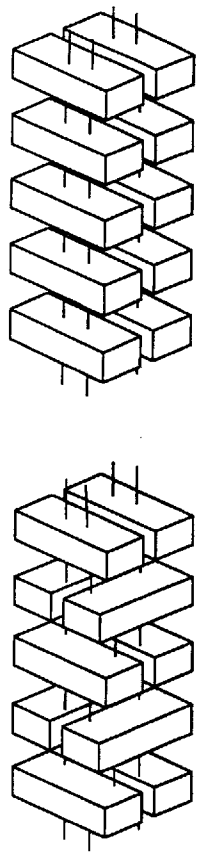

Figure 6. (*a*) Schematic representation of model 1 as a tilted side view of a line drawing showing the relative positions of pairs of **DA-*n*** molecules within a column; (*b*) schematic representation of model 2 as a tilted side view of a line drawing showing the relative positions of pairs of **DA-*n*** molecules within a column. Each parallelepiped represents one **DA-*n*** molecule and the connecting vertical lines represent the H-bonds.

The average thickness of the AB double layer in model 2 is 9·2 Å, which fits well with the *c*-dimension of the hexagonal crystal unit cell in **DA-5**. The ABBA stacking of layers in model 2 is thus an attractive proposition also from the point of view of the similarity with **DA-5**. However, as mentioned earlier the existence of the 0 0 3 reflection in **DA-5** crystals means that the two layers differ by more than a simple rototranslation.

4. Conclusions

The diamides **DA-*n*** with alkyl chains containing small numbers of methylenic units (n=4, 4/1*, 5, 6, and 7) form only crystalline phases. In contrast, diamides with

Downloaded At: 09:01 26 January 2011

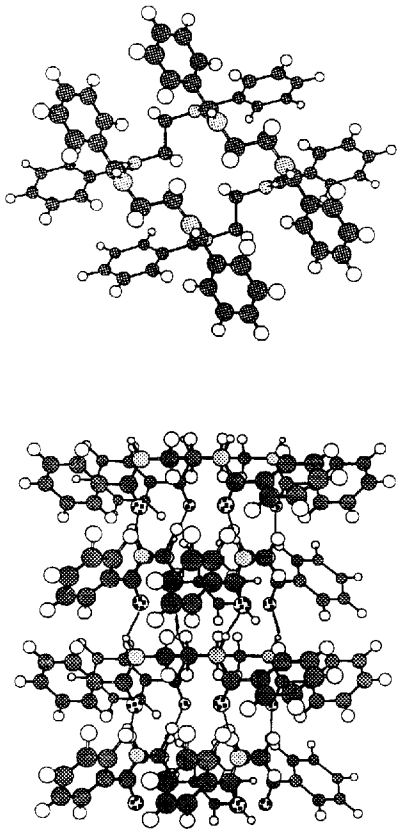

Figure 7. (*a*) Ball and stick top view of a two layer cross-section of the column from figure 6(*b*); (*b*) ball and stick side view of the column from figure 6(*b*). The alkyl groups of **DA-*n*** molecules are not shown.

long alkyl chains ($n=10$, 11, 12, 14, 16 and 18) self-assemble to form a supramolecular column which displays a hexagonal columnar liquid crystalline phase above the crystal melting point. The ability of long-chain diamides to form the 2-D columnar phase confirms the role of flexible chains in decoupling translational register between adjacent columns. *All experimental data are consistent with a model in which the melted outstretching alkyl chains occupy a space of constant density surrounding the rigid H-bonded amide channel which forms a hexagonal lattice.* Local ABAB stacking of layers containing two dimer molecules each is proposed along the column, with layer B rotated by 90° around the column axis relative to layer A.

The high temperature crystalline phase of **DA-*n*** with $n=4$, 5, 6 and 7 is nearly hexagonal. The low temperature crystal form of **DA-5** is truly hexagonal, with $a=24{\cdot}9$ ($\pm 0{\cdot}3$) Å, $c=9{\cdot}4$ ($\pm 0{\cdot}2$) Å and contains four molecules per unit cell. The three-fold or six-fold molecular site symmetry indicates that the crystal is orientationally disordered. The most likely arrangement in this crystal structure is one in which two molecular pairs of a unit cell are located above each other on a six-fold axis producing a structure similar to that suggested for the columnar phase.

Financial support by the National Science Foundation (DMR-92-06781 and DMR-91-22227), the Engineering and Physical Science Research Council, U.K., and a NATO travelling grant are gratefully acknowledged. We also thank Professor S. Z. D. Cheng of the University of Akron for performing the density measurements and Dr K. Gardner of the Central Research and Development, Experimental Station, DuPont, Wilmington, DE for providing the single crystal structure of **DA-1** prior to publication.

Appendix

The diffraction data for the low temperature crystal form of the **DA-5** in table 6 shows that there are no systematic absences. This leaves a choice of eight possible space groups: *P*6, *P*$\bar{6}$, *P*6*m*, *P*622, *P*6*mm*, *P*$\bar{6}$*m*2, *P*$\bar{6}$2*m*, and *P*6/*m*2/*m*2/*m*. On the other hand, density data allow only $m=N=4$ nonequivalent positions in the unit cell, or in the case of molecular pair formation, only $m=N/2=2$ positions. In the case of $m=4$, irrespective of the space group, the molecules would be placed at special positions (1/3 2/3 z, 2/3 1/3 z, 1/3 2/3 $\bar{z}$, and 2/3 1/3 $\bar{z}$ in figure 6(*a*); each solid circle represents 2 sites, 1 at z and the other at $\bar{z}$). In *P*6/*m*, *P*622, and *P*$\bar{6}$2, these sites have the symmetry of a three-fold axis (i.e. 3), and in *P*6/*m*2/*m*2/*m* that of a three-fold axis and a mirror plane along it (i.e. 3*m*).

In the case of $m=2$ positions per unit cell, each being associated with the centre of a molecular pair, there are several possibilities. Firstly, the 2 pairs can lie either above each other or side by side. In the latter case the coordinates of the 2 positions are either (1/3 2/3 z, 2/3 1/3 z), or (1/3 2/3 0, 2/3 1/3 0), or (1/3 2/3 1/2, 2/3 1/3 1/2) (see figure 6(*a*)), where each solid circle now represents only 1 site, i.e. the centre of the molecular pair. In none of these side by side configurations does the special position have six-fold symmetry (site symmetries are 3, $\bar{z}$, 32, 3*m* or $\bar{6}$*m*2). Each site has 3 nearest neighbours in the basal plane. On the other hand, where the 2 special positions are located above each other, the coordinates are either (2/3 1/3 z, 2/3 1/3 $\bar{z}$) or (1/3 2/3 z, 1/3 2/3 $\bar{z}$) (see figure 6(*b*) and (*c*) respectively) or else (0 0 z, 0 0 $\bar{z}$) (see figure 6(*d*)).

It can be noted from the above discussion that all the available lattice sites have at least three-fold symmetry, whereas any particular conformation of the diamide molecule or molecular pair can at best have only two-fold symmetry. This implies that the crystal is orientationally and possibly also conformationally disordered, the lattice site thus matching the symmetry of the

Downloaded At: 09:01 26 January 2011

rotationally averaged molecule. This being the case, and in view of the dimeric nature of either the molecule or molecular pair, six-fold symmetry appears more likely than three-fold symmetry. As already mentioned, six-fold symmetry would necessitate the arrangement of molecular pairs on top of one another as shown in figure 6(*d*). This arrangement is the closest to the one normally envisaged for the hexagonal columnar phase. The absence of the 0 0 1 reflection would suggest that z is close to 1/2.

Further considerations which tend to disfavour both side by side arrangements of molecular pairs ($m=2$) and the $m=4$ case, both depicted in figure 6(*a*) are the following:

- This arrangement (see figure 6(*a*) provides a less effective phase separation between polar and non-polar moieties than that in figure 6(*b*), (*c*) and (*d*).
- Hydrogen bonding can only be established within molecular pairs where the in plane distance of $a/(3)^{1/2}=14$ Å between pairs is too large. In contrast, the alternative arrangement (see figure 6(*b*), (*c*) and (*d*)) allows clustering of all 4 molecular centres belonging to a unit cell, thus potentially allowing both in-plane and out of plane H-bonding.
- Each molecule or pair has only 3 rather than 6 nearest neighbours. Hence this arrangement differs substantially from that in the hexagonal columnar phases, and the observed continuity of lattice parameter a versus alkyl tail length between **DA-5** and higher amides (see figure 4(*a*)) would not be expected, except through coincidence. In addition, as already mentioned, there is no obvious reason for three-fold rather than a six-fold site symmetry in an orientationally-disordered crystal of dimeric molecules.

In conclusion, the most likely arrangement in the low-temperature crystal of **DA-5** is that represented in figure 6(*d*) where pairs of dimer molecules are centred on a six-fold axis above each other.

Downloaded At: 09:01 26 January 2011

References

[1] For some general review articles on self-assembly and other aspects of supramolecular chemistry see: (*a*) LEHN, J.-M., 1988, *Angew. Chem. Int. Ed. Engl.*, **27**, 89; (*b*) LEHN, J.-M., 1990, *Angew. Chem. Int. Ed. Engl.*, **29**, 1304; (*c*) LINDSEY, J. S., 1991, *New J. Chem.*, **15**, 153; (*d*) WHITESIDES, G. M., MATHIAS, J. P., and SETO, C. T., 1991, *Science*, **254**, 1312; (*e*) LEHN, J.-M., 1993, *Makromol. Chem., Macromol. Symp.*, **69**, 1.

[2] For a few recent books on supramolecular chemistry see: (*a*) SCHNEIDER, H. J., and DURR, H. (Eds), 1991, *Frontiers in Supramolecular Organic Chemistry and Photochemistry* (New York: VCH); (*b*) BALZANI, V., and DE COLA, L., (Eds.), 1991, *Supramolecular Chemistry* (Boston: Kluwer Academic Publ.), (*c*) VÖGTLE, F., 1991, *Supramolecular Chemistry* (New York: J. Wiley and Sons); (*d*) Ciba Foundation Symposium 158, *Host–Guest Molecular Interactions: From Chemistry to Biology* (New York: J. Wiley and Sons); (*e*) WEBER, E. (Ed.), 1993, *Supramolecular Chemistry. I. Directed Synthesis and Molecular Recognition, Top. Curr. Chem.*, **165**; (*f*) PERCEC, V., and TIRRELL, D. A. (Eds), 1994, *New Macromolecular Architecture and Supramolecular Polymers, Macromol. Symp.*, **77**.

[3] For some selected examples of supramolecular shapes which display calamitic liquid crystalline phases see: (*a*) low molar mass mesogens: HOFFMANN, S., WITKOWSKI, W., BORRMANN, G., SCHUBERT, H., and WIESSFLOG, W., 1978, *Z. Chem.*, **18**, 403; KATO, T., and FRÉCHET, J. M. J., 1989, *J. Am. chem. Soc.*, **111**, 8533; (*b*) side chain liquid crystalline polymers: KUMAR, U., KATO, T., and FRÉCHET, J. M. J., 1992, *J. Am. chem. Soc.*, **114**, 6630; (*c*) main chain liquid crystalline polymers: BLADON, P., and GRIFFIN, A. C., 1993, *Macromolecules*, **26**, 6604; KOTERA, M., LEHN, J.-M., and VIGNERON, J.-P., 1994, *J. chem. Soc., chem. Commun.*, 197; (*d*) liquid crystalline networks: KATO, T., KIHARA, H., KUMAR, U., URYU, T., and FRÉCHET, J. M. J., 1994, *Angew. Chem. Int. Ed. Engl.*, **33**, 1644; WILSON, L. M., 1994, *Macromolecules*, **27**, 6683.

[4] For some selected examples of supramolecular shapes which display columnar hexagonal liquid crystalline phases see: (*a*) disc-like mesogens: BRIENNE, M.-J., GABARD, J., LEHN, J.-M., and STIBOR, I., 1989, *J. chem. Soc., chem. Commun.*, 1868; CIUCHI, F., DI NICOLA, G., FRANZ, H., GOTTARELLI, G., MARIANI, P., BOSSI, M. G. P., and SPADA, G. P., 1994, *J. Am. chem. Soc.*, **116**, 7064; LATTERMAN, G., STAUFER, G., and BREZESINSKI, G., 1991, *Liq. Cryst.*, **10**, 169; (*b*) supramolecular cylinders: FOUQUEY, C., LEHN, J.-M., and LEVELUT, A.-M., 1990, *Adv. Mater.*, **2**, 254; KRZYWICKI, T. G., FOUQUEY, C., and LEHN, J.-M., 1993, *Proc. Natl. Acad. Sci. USA*, **90**, 163; XU, B., SWAGER, T. M., 1995, *J. Am. chem. Soc.*, **117**, 5011.

[5] See the review: PERCEC, V., and JOHANSSON, G., *Molecular, Macromolecular and Supramolecular Liquid Crystals Containing Macroheterocyclic Ligands*, in *Macromolecular Design of Polymeric Materials*, (edited by K. HATADA, T. KITAYAMA and O. VOGL (New York: Marcel Dekker), (in the press).

[6] For some recent reviews on metallomesogens see: (*a*) HUDSON S. A., and MAITLIS, P. M., 1993, *Chem. Rev.*, **93**, 861; (*b*) POLISHCHUK, A. P., and TIMOFEEVA, T. V., 1993, *Russ. Chem. Rev.*, **62**, 291; (*c*) ESPINET, P., ESTERUELAS, M. A., ORO, L. A., SERRANO, J. L., and SOLA, E., 1992, *Coord. Chem. Rev.*, **117**, 215; (*d*) GIROUD-GODQUIN, A.-M., and MAITLIS, P. M., 1991, *Angew. Chem. Int. Ed. Engl.*, **30**, 375; (*e*) ORIOL, L., and SERRANO, J. L., 1995, *Adv. Mater.*, **7**, 348.

[7] For examples of various disc-like structures reported from our laboratory see: (*a*) PUGH, C., and PERCEC, V., 1991, *J. mater. Chem.*, **1**, 765; (*b*) PERCEC, V., CHO, C. G., and PUGH, C., 1991, *Macromolecules*, **24**, 3227; (*c*) PERCEC, V., CHO, C. G., and PUGH, C., 1991, *J. mater. Chem.*, **1**, 217.

[8] For a few examples of semi-flexible main chain polymers see: (*a*) UNGAR, G., FEIJO, J. L., PERCEC, V., and YOURD, R., 1991, *Macromolecules*, **24**, 953; PERCEC, V.,

ZUBER, M., UNGAR, G., and ALVAREZ-CASTILLO, A., 1992, *Macromolecules*, **25**, 439; (*b*) for an example of hyperbranched polymer with flexible disc-like mesogens see: PERCEC, V., CHO, G. C., PUGH, C., and TOMAZOS, D., 1992, *Macromolecules*, **25**, 1164; (*c*) for examples of polymers with tapered side groups see: PERCEC, V., HECK, J., and UNGAR, G., 1991, *Macromolecules*, **29**, 4957; PERCEC, V., LEE, M., HECK, J., BLACKWELL, H., UNGAR, G., and ALVAREZ-CASTILLO, A., 1991, *J. mater. Chem.*, **2**, 931; PERCEC, V., HECK, J., LEE, M., UNGAR, G., and ALVAREZ-CASTILLO, A., 1992, *J. Mater. Chem.*, **2**, 1033.

[9] (*a*) PERCEC, V., JOHANSSON, G., HECK, J., UNGAR, G., and BATTY, S. B., 1993, *J. chem. Soc. Perkin Trans. 1*, 1411; (*b*) JOHANSSON, G., PERCEC, V., UNGAR G., and ABRAMIC, D., 1994, *J. chem. Soc. Perkin Trans. 1*, 447; (*c*) PERCEC, V., HECK, J., TOMAZOS, D., FALKENBERG, F., BLACKWELL, H., and UNGAR, G., 1993, *J. chem. Soc. Perkin Trans. 1*, 2799; (*d*) PERCEC, V., HECK, J. A., TOMAZOS, D., and UNGAR, G., 1993, *J. chem. Soc. Perkin Trans. 2*, 2381; (*e*) PERCEC, V., TOMAZOS, D., HECK, J., BLACKWELL, H., and UNGAR, G., 1994, *J. chem. Soc. Perkin Trans. 2*, 31; (*f*) TOMAZOS, D., OUT, G., HECK, J. A., JOHANSSON, G., PERCEC, V., and MOELLER, M., 1994, *Liq. Cryst.*, **16**, 509; (*g*) UNGAR, G., BATTY, S. V., PERCEC, V., HECK, J., and JOHANSSON, G., 1994, *Adv. Mater. Opt. Electr.*, **4**, 303.

[10] For few brief reviews of our research on supramolecular columns see: (*a*) PERCEC, V., HECK, J., JOHANSSON, G., and TOMAZOS, D., 1994, *Macromol. Symp.*, **77**, 237; (*b*) PERCEC, V., HECK, J., JOHANSSON, G., TOMAZOS, D., KAWASUMI, M., and UNGAR, G., 1994, *J. Macromol. Sci.—Pure Appl. Chem.*, **A31**, 1031; (*c*) PERCEC, V., HECK, J., JOHANSSON, G., TOMAZOS, D., KAWASUMI, M., CHU, P., and UNGAR, G., 1994, *J. Macromol Sci.—Pure Appl. Chem.*, **A31**, 1719; (*d*) PERCEC, V., HECK, J., JOHANSSON, G., TOMAZOS, D., KAWASUMI, M., CHU, P., and UNGAR, G., 1994, *Mol. Cryst. liq. Cryst.*, **254**, 137.

[11] For some references on the columnar mesophases exhibited by biological compounds see: (*a*) YEVDOKIN, YU., M., SKURIDIN, S. G., and SALYANOV, V. I., 1988, *Liq. Cryst.*, **3**, 1443; LIVOLANT, F., LEVELUT, A. M., DOUCET, J., and BENOIT, J. P., 1989, *Nature*, **339**, 724; LEFORESTIER, A., and LIVOLANT, F., 1994, *Liq. Cryst.*, **17**, 651; REICH, Z., WACHTEL, E. J., and MINSKY, A., 1994, *Science*, 264, 1460; (*b*) DNA, peptides and xanthan: LIVOLANT, F., and BOULIGAND, Y., 1986, *J. Phys.*, **47**, 1813; (*c*) other biological liquid crystals: BROWN, H. G., and WOLKEN, J. J., 1979, *Liquid Crystals and Biological Structures* (New York: Academic Press).

[12] For a few selected review articles on columnar mesophases displayed by various classes of compounds see: (*a*) disc-like mesogens: CHANDRASEKHAR, S., and RANGANATH, G. S., 1990, *Rep. Prog. Phys.*, **53**, 57; (*b*) phasmids and polycatenar mesogens: MALTHÊTE, J., NGUYEN, H. T., and DESTRADE, C., 1993, *Liq. Cryst.*, **13**, 171; (*c*) amphiphilic compounds: SKOULIOS, A., and GUILLON, D., 1988, *Mol. Cryst. liq. Cryst.*, **165**, 317; (*d*) low molar mass mesogens with various shapes: DEMUS, D., 1989, *Liq. Cryst.*, **5**, 75; (*e*) polymers: UNGAR, G., 1993, *Polymer*, **34**, 2050; GODOVSKY, YU, K., and PAPKOV, V. S., 1989, *Adv. Polym. Sci.*, **88**, 129; PERCEC, V., and TOMAZOS, D., 1992, *Comprehensive Polymer Science*, First Suppl., edited by G. ALLEN (Oxford: Pergamon Press) p. 299; (*f*) lyotropic systems; LUZZATI, V., 1958, *Discuss. Faraday Soc.*, **25**, 43.

[13] GARDNER, K., Central Research, Experimental Station, DuPont, personal communication of unpublished results.

[14] (*a*) SCHEINER, S., and WANG, L., 1993, *J. Am. chem. Soc.*, **115**, 1958; (*b*) STICKLE, D. F., PRESTA, L. G., DILL, K. A., and ROSE, G. D., 1992, *J. Mol. Biol.*, **226**, 1143; (*c*) DOIG, J. D., and WILLIAMS, D. H., 1992, *J. Am. chem. Soc.*, **114**, 338; (*d*) CHIDAMBARAM, R., and RAMANADHAM, M., 1991, *Physica B*, **174**, 300; (*e*) MITCHELL, J. B. O., and PRICE, S. L., 1991, *Chem. Phys. Lett.*, **180**, 517; (*f*) GELLMAN, S. H., DADO, G. P., LIANG, G. B., and ADAMS, B. R., 1991, *J. Am. chem. Soc.*, **113**, 1164; (*g*) SNEDDON, S. F., TOBIAS, D. J., and BROOKS III, C. L., 1989, *J. Mol. Biol.*, **209**, 817; (*h*) MITCHELL, J. B. P., and PRICE, S. L., 1989, *Chem. Phys. Lett.*, **154**, 267; (*i*) TRIGGS, N. E., BONN, R. T., and VALENTINI, J. J., 1993, *J. phys. Chem.*, **97**, 5535; (*j*) SEARLE, M. S., WILLIAMS, D. H., and GERHARD, U., 1992, *J. Am. chem. Soc.*, **114**, 10697; (*k*) LEISEROWITZ, L., and HAGLER, A. T., 1983, *Proc. R. Soc. Lond. A.*, **388**, 133; (*l*) LEISEROWITZ, L., and TUVAL, M., 1978, *Acta. Cryst.*, B34, 1051; (*m*) LIANG, G. B., DESPER, J. M., and GELLMAN, S. H., 1993, *J. Am. chem. Soc.*, **115**, 925.

[15] (*a*) BRISSON, J., and BRISSE, F., 1989, *Macromolecules*,, **22**, 1974; (*b*) PALMER, P. A., and BRISSE, F., 1980, *Acta Crystallogr.*, **B36**, 1447; (*c*) BRISSON, J., GAGNE, J., and BRISSE, F., 1989, *Can. J. Chem.*, **67**, 840; (*d*) BRISSON, J., and BRISSE, F., 1986, *Macromolecules*, **19**, 2633.

[16] MALTHETE, J., LEVELUT, A. M., and LIEBERT, L., 1992, *Adv. Mater.*, **4**, 37.

Downloaded At: 09:01 26 January 2011